

## EFFECTS OF TIME-DELAY ON ONE-DIMENSIONAL NONLINEAR ACOUSTICS

PACS No. 43.25.-x

J. I. Ramos

Escuela de Ingenierías, Universidad de Málaga, Dr. Ortiz Ramos, s/n, 29071 Málaga, Spain,  
Tel. 951952387, Fax 951952452, e-mail: jirs@lcc.uma.es

### ABSTRACT

The effects of stress relaxation on one-dimensional nonlinear acoustics are analyzed by considering a viscous Burgers' equation with time delay. It is shown that, for small delays, a Taylor's series expansion to first order results in a nonlinear equation analogous to that of the regularized long-wave equation which is solved asymptotically by means of a regular perturbation technique. Both the asymptotic and the numerical solution of the time-delayed Burgers' equation are shown to be in agreement with each other and indicate that the time delay affects the shock wave development and curvature. For large time delays, it is shown that a solitary wave may be formed and that substantial radiation may result depending on the initial conditions.

**Keywords:** relaxation, Burgers' equation, nonlinear wave propagation.

### 1 Introduction

The one-dimensional Burgers' equation, i.e.,

$$u_t(t, x) + u(t, x) u_x(t, x) = \sigma_x(t, x), \quad (1)$$

where  $u$ ,  $t$  and  $x$  denote the velocity, time and spatial coordinate, respectively,  $\sigma = \mu u_x$  is the (Newtonian) stress and  $\mu$  is the (kinematic) viscosity coefficient, has been used frequently in many branches of fluid dynamics for the study of turbulence [1,2], traffic flow, acoustics, etc. [3,4]. The inviscid Burgers' equation, i.e., Eq. (1) with  $\mu = 0$ , has an analytical solution and may result in the formation of shock waves, depending on the initial conditions; on the other hand, the viscous Burgers' equation, i.e., Eq. (1) with  $\mu \neq 0$ , may be solved analytically by means of the Cole-Hopf transformation [5,6] which transforms it into a linear heat transfer equation. The viscous Burgers' equation exhibits steepening for small values of the viscosity coefficient, and the steepness increases as  $\mu$  is decreased.

In this paper, we shall be concerned with

$$u_t(t, x) + u(t, x) u_x(t, x) = \sigma_x(t, x), \quad \sigma(t, x) = \mu u_x(t + \tau, x), \quad (2)$$

where  $\tau$  is a time delay or lag. Equation (2) reduces to Eq. (1) for  $\tau = 0$ . For  $|\tau| \ll 1$ , a Taylor's series expansion of the right-hand side of Eq. (2) about  $(t, x)$  yields

$$u_t + u u_x = \mu u_{xx} + \delta u_{xxt} + O(\tau^2), \quad (3)$$

where  $\delta = \mu \tau$ . Equation (2) with  $\mu = 0$  is usually referred to as the regularized long-wave equation [7] and is a model for describing long-wave behavior and the formation of undular bores, the study of non-linear dispersive waves, shallow water waves, ion acoustic plasma waves, etc. It must be noted that Eq. (2) indicates that a velocity gradient at  $(t + \tau, x)$  results in a stress at  $(t, x)$  and that we have assumed that  $\tau$  is positive. If  $\tau$  were negative, then a time translation, followed by a Taylor' series expansion of Eq. (2) would result in a nonlinear second-order wave equation which will not be considered in this study; such an equation is a bit more complex than the one derived by Fay [8] to study the propagation of finite-amplitude, acoustic plane waves. Both Eq. (3) and Fay's Eq. (4) include a third-order mixed derivative, i.e., the second term in the right-hand side of Eq. (3).

In previous studies that have considered relaxation effects on acoustics and shock wave structure, authors have considered only a single relaxation process and applied the operator  $(1 + \tau \partial/\partial t)$  to the original (unrelaxed) equations [9-12]. Such an approach is analogous to the inversion of the same operator in the formulation described above, but introduces a second-order time derivative, thereby transforming the original parabolic equation into a hyperbolic one unless certain approximations are made to neglect such a derivative. By way of contrast, the approach proposed here is based on the assumption that there is a time delay between the stress and velocity gradient and does not result in an increase on the order of the time derivative.

## 2 Asymptotic analysis

If in Eq. (3), the  $O(\tau^2)$  are neglected and  $\delta \ll 1$ , it may be assumed that the resulting equation can be solved by means of the following regular perturbation expansion

$$u(t, x) = u_0(t, x) + \delta u_1(t, x) + O(\delta^2), \quad (4)$$

which upon substitution into Eq. (3) yields, at leading-order in  $\delta$ ,

$$u_{0,t} + u_0 u_{0,x} = \mu u_{0,xx}, \quad (5)$$

i.e., the viscous Burgers' equation, whereas at  $O(\tau^1)$ , one can easily derive

$$u_{1,t} + u_0 u_{1,x} + u_1 u_{0,x} = \mu u_{1,xx} + u_{0,xxt}, \quad (6)$$

which is a linear second-order partial differential for  $u_1$  forced by  $u_{0,xxt}$  and whose coefficients depend on the leading-order solution  $u_0(t, x)$ . Equation (6) is a linear generalized regularized-long wave (GRLW) equation [13]. Although, Eq. (5) may be solved analytically in some cases by means of, for example, the Cole-Hopf transformation, the dependence of the coefficients of Eq. (6) on space and time makes it difficult to solve this equation analytically.

In Eq. (5), the nonlinear terms cause steepness, whereas the viscous ones cause dissipation. This is clearly shown in the dispersion relation for the linearized Eq. (5), i.e.,  $u_{0,t} + v u_{0,x} = \mu u_{0,xx}$ , which may be written as

$$i \omega = ik v + \mu k^2, \quad (7)$$

where  $i^2 = -1$ ,  $u(t, x) = A \exp(i(kx - \omega t))$ , and  $A$ ,  $\omega$  and  $k$  are the amplitude, frequency and wavenumber, respectively. For real wave numbers, the angular frequency is a complex number whose real and imaginary parts are  $\omega_R = k v$  and  $\omega_I = -\mu k^2$ , respectively, so that  $u(t, x) = A \exp(\omega_R t) \exp(i(kx - \omega_R t))$ , and the amplitude decreases with time owing to the viscosity, while the phase speed is  $v$ . On the other hand, a similar linearized analysis of Eq. (3) yields the following dispersion relation

$$i \omega (1 + \delta k^2) = ik v + \mu k^2, \quad (8)$$

which for positive  $\delta$ , yields  $\omega_R = k v / (1 + \delta k^2)$  and  $\omega_I = -\mu k^2 / (1 + \delta k^2)$  and the damping increases as the wavenumber is increased; there is no damping for a wavenumber equal to zero and the largest damping occurs as the wavenumber tends to infinity and is asymptotic to  $\mu / \delta$ . On the other hand, the phase speed is  $v / (1 + \delta k^2)$  and tends to zero as the wavenumber approaches infinity. Moreover, Eq. (3) is a dispersive wave equation which in the absence of viscosity may result in the formation of solitons when the nonlinearities balance the dispersion term [13]. It must be noted that when considering Eq. (3), we have treated  $\mu$  and  $\delta$  as independent parameters, even though our derivation of such an equation was based on Taylor's series expansion and, therefore,  $\delta = \mu \tau$ .

### 3 Numerical methods and boundary conditions

Equation (3) can be written as the following system of equations

$$u_t \equiv v, \quad v + u u_x = \mu u_{xx} + \delta v_{xx}, \quad (9)$$

which clearly indicates that  $u$  and  $v$  are nonlinearly coupled and could be determined iteratively by means of, for example, finite difference methods. Since the second Eq. (9) is linear in  $v$ , one could also solve this equation analytically in a piecewise manner and then solve the first Eq. (7) to obtain  $u$  [13,14]; however, the resulting finite difference method, albeit locally exact, has an accuracy that depends on the discretization of the first- and second-order spatial derivatives of  $u$ . Moreover, since in the absence of dispersion, Eq. (3) is characterized by steep moving fronts whose steepness increases as the viscosity is decreased, we have developed the following fourth-order accurate method in both space and time. The first Eq. (9) is solved in time by means of a fourth-order accurate Runge-Kutta method whose four stages require the value of  $v$ ; therefore, at each stage, one has to solve the second Eq. (9) which was discretized as follows. From the initial conditions and by defining  $F \equiv u_x$  and  $G \equiv u_{xx}$ , one can easily determine the nodal values of  $F$  and  $G$  by solving the two following tridiagonal systems of linear algebraic equations

$$(G_{i-1} + 10 G_i + G_{i+1})/12 = (u_{i-1} - 2u_i + u_{i+1})\Delta x^2 + O(\Delta x^4), \quad (10)$$

$$(F_{i-1} + 4 F_i + F_{i+1})/6 = (u_{i+1} - u_{i-1})/(2\Delta x) + O(\Delta x^4), \quad (11)$$

which correspond to a three-point, fourth-order accurate, compact operator method discretization of the second- and first-order derivatives, respectively [15], where the subscript  $i$  denotes the  $i$ -th grid point, i.e.,  $x_i = i \Delta x$ .

The second Eq. (9) can be written as

$$v - \delta v_{xx} = \mu u_{xx} - u u_x = \mu G - u F \equiv S \equiv v - \delta H, \quad (12)$$

which, upon using a similar fourth-order accurate discretization to Eq. (10), provides the nodal values of  $v$ , and, therefore, a fourth-order accurate discretization of the spatial derivatives. Therefore, the method of lines described in this section requires at each stage of the fourth-order accurate Runge-Kutta method the solution of three systems of tridiagonal matrices for the determination of  $F$ ,  $G$  and  $v$ , and due to its explicit character and the compact discretization of the first- and second-order spatial derivatives is subject to stability restrictions that depend on the Courant, Fourier and dispersion numbers, i.e.,  $v \Delta t / \Delta x$ ,  $\mu \Delta t / \Delta x^2$ , and  $\delta / \Delta x^2$ , respectively, where  $v$  is a characteristic value of  $u$ .

In addition to the fourth-order accurate method described in previous paragraphs, the following implicit, exponential technique has also been used. Equation (12) can be approximated in the interval  $[x_{i-1}, x_{i+1}]$  by

$$v - \delta v_{xx} = S_i, \quad (13)$$

which can be solved analytically in that interval subject to the conditions  $v(x_{i-1}) = v_{i-1}$ ,  $v(x_i) = v_i$  and  $v(x_{i+1}) = v_{i+1}$  to obtain a piecewise exponential solution, whereas the first Eq. (9) was discretized by means of a  $\theta$ -method as

$$(u_i^{n+1} - u_i^n) / \Delta t = \theta v_i^{n+1} + (1 - \theta)v_i^n, \quad (14)$$

where the superscript  $n$  denotes the  $n$ -th time level, i.e.,  $t^n = n \Delta t$ . Equation (14) results in an explicit, first-order accurate method for  $\theta = 0$ , and implicit, first- and second-order accurate techniques for  $\theta = 1$  and  $\theta = 1/2$ , respectively. However, implicit methods require the use of iterative methods for their solution due to the nonlinear dependence of  $v$  upon  $u$  and its second-order spatial derivatives. It must also be noted that the spatial fourth-order discretizations presented above can also be used together with Eq. (14) to obtain the numerical solution, but this technique would also require an iterative procedure and would be more costly than the exponential method just described because it does require the solution of two systems of tridiagonal matrices at each iteration, whereas the exponential method described above requires only the solution of a tridiagonal system at each time step. Iterations may be avoided altogether by linearizing Eq. (3) at each time level and solving the resulting linear equations by means of either the fourth-order compact or the exponential method described in this section.

#### 4 Presentation of results

Figure 1 illustrates the numerical solution corresponding to  $\mu = 0.001$  and  $\delta = 0$  and an initial condition  $u(0, x) = a \exp(-b(x - c)^2)$  with  $a = 0$ ,  $b = 30$  and  $c = 0.5$ , and homogeneous Dirichlet boundary conditions, and shows the evolution from a bell-shaped profile to the formation of a steep shock front whose thickness is not zero on account of the small (but different from zero) viscosity coefficient employed in the study. Although not clearly visible in Figure 1, the maximum pressure decreases as time increases on account of the viscosity.

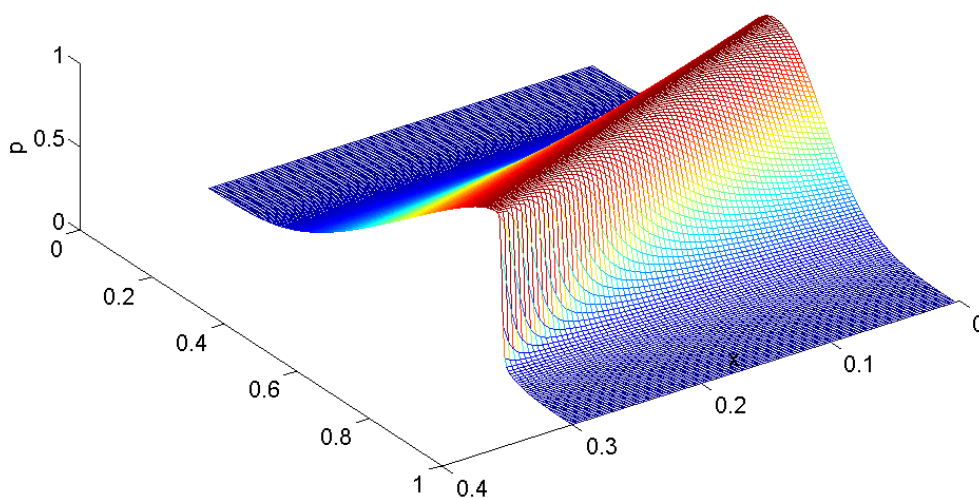


Figure 1 – Acoustic pressure field as a function of space and time for Dirichlet's boundary conditions,  $\mu = 0.001$  and  $\delta = 0$ , and a Gaussian initial condition

For the same values of the parameters as those of Figure 1 but  $\delta = 0.01$ , the results presented in Figure 2 indicate that a shock wave is formed at the advancing front whereas the rear of the wave exhibits an almost linear behavior as a function of the spatial coordinate. Although not shown here, the results presented in Figure 2 are entirely similar to those presented in Figure 1 and those corresponding to  $\delta = 0.1$ , i.e., for dispersion parameters which are larger than the viscosity, thus indicating that for the conditions considered in Figures 1 and 2, the asymptotic analysis presented previously in this paper is valid even for values of  $\delta = 0.1$ , thus confirming both the validity of both the second-order approximation and the numerical results. It should also be noted that no oscillations are observed in the numerical results illustrated in Figures 1 and 2.

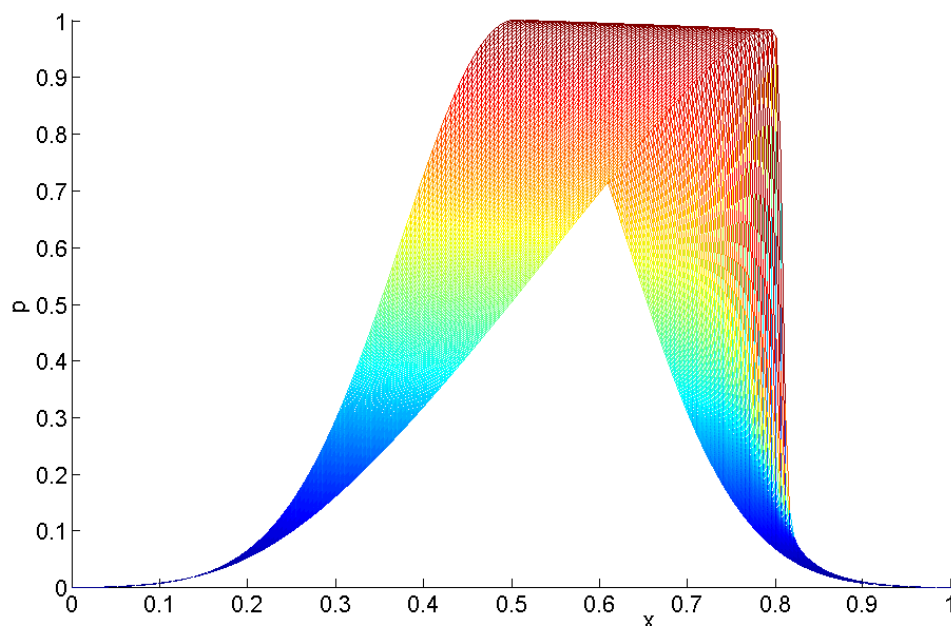


Figure 2 – Acoustic pressure field as a function of space and time for Dirichlet's boundary conditions,  $\mu = 0.001$  and  $\delta = 0.01$ , and a Gaussian initial condition

Similar results to those presented in Figures 1 and 2 have also been obtained for the following sinusoidal condition  $u(0, x) = \sin(\pi x)$  and some are shown in Figure 3 which exhibits similar trends to those discussed above until the shock wave reaches the downstream boundary. Beyond that time, the results are not valid, although they are shown in Figure 3 in order to illustrate the robustness of the numerical methods presented here as well as the non-physical effects that occur when the computations are extended beyond the time at which the shock wave strikes the downstream boundary. Despite the numerical robustness and the absence of oscillations, the results illustrated in Figure 3 clearly indicate that the maximum amplitude decreases with time and that the tail is a linear function of space, once the shock wave reaches the downstream boundary.

Although not shown here, as the viscosity coefficient is increased, the wave's maximum amplitude decreases, the width increases, and a shock wave may not form. On the other hand, as the dispersion parameter is increased, a balance may be reached between the nonlinear convective terms and the dispersion ones and, then, a solitary wave solution may appear. In the absence of viscosity, these solitary waves are solutions of the equal-width, regularized-long wave and generalized regularized-long wave equations [13,14].

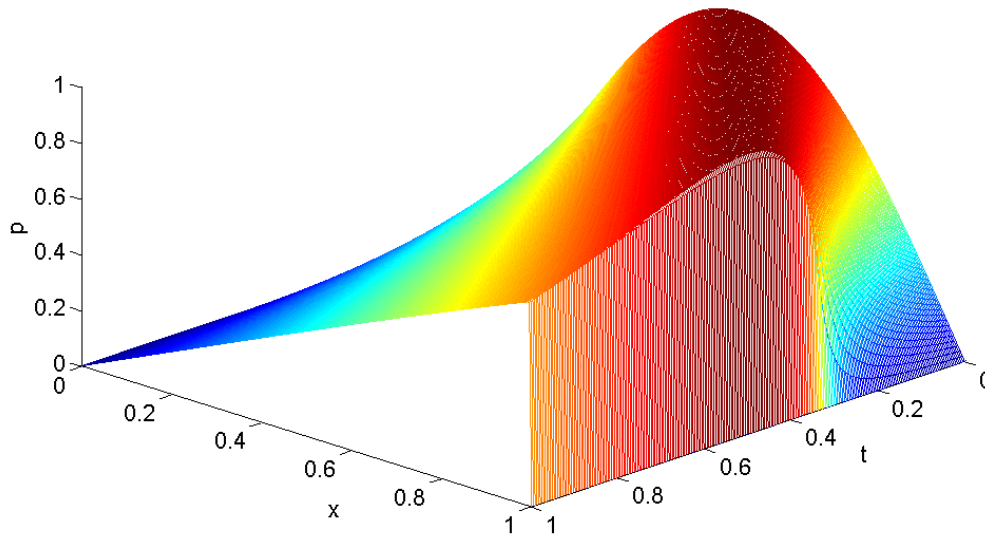


Figure 3 – Acoustic pressure field as a function of space and time for Dirichlet's boundary conditions,  $\mu = 0.001$  and  $\delta = 0$ , and a sinusoidal initial condition

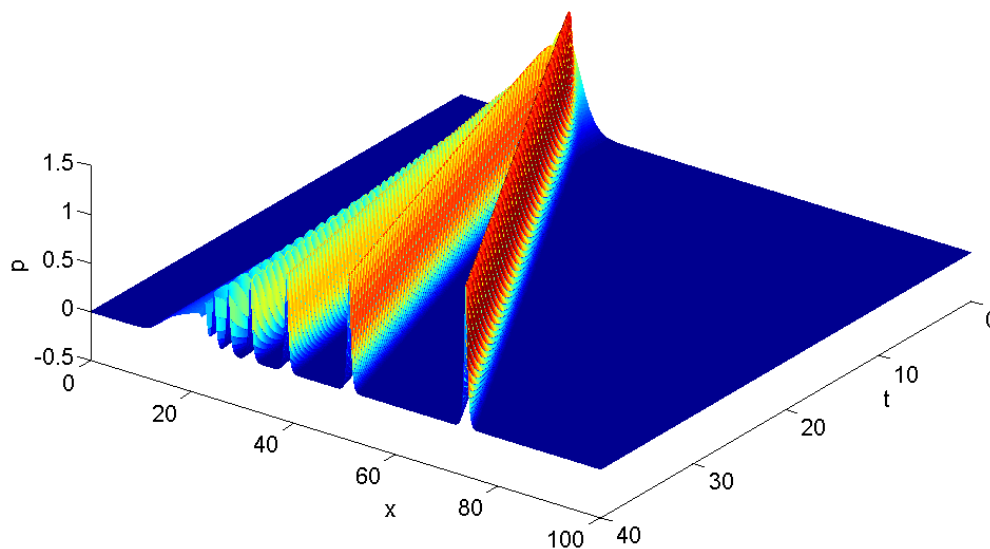


Figure 4 – Acoustic pressure field as a function of space and time for Dirichlet's boundary conditions,  $\mu = 0$  and  $\delta = 0.1$ , and a Gaussian initial condition characterized by  $a = 0$ ,  $b = 0.1$  and  $c = 20$

Figure 4 illustrates the acoustic field for an initial Gaussian pressure distribution in the presence of dispersion/relaxation but not viscosity. The initial conditions considered in this figure do not correspond to the exact solution of Eq. (3) in the absence of viscosity and, as a consequence, there is an initial transient whereby the wave undergoes a transformation that results in the

formation of several solitary waves that move apart from each other and that preserve their integrity. The first generated wave is the one with the largest amplitude; the amplitudes of the waves decrease as their generation times increase. The back of the last wave exhibits a steep front followed by a smooth transition to the upstream boundary condition, thus suggesting that these solitary waves are formed as a consequence of the steepness caused by the nonlinear convection terms which, eventually, are balanced out by dispersion. Figure 4 also shows that the initial conditions employed in this study results in the formation of a fan of solitary waves which do not interact with and separate from each other as time increases. It must be noted that, if the initial condition corresponded to the exact solution of Eq. (3), then only one solitary wave would have been formed in accordance with previous theoretical and numerical results for the regularized long-wave equation [14].

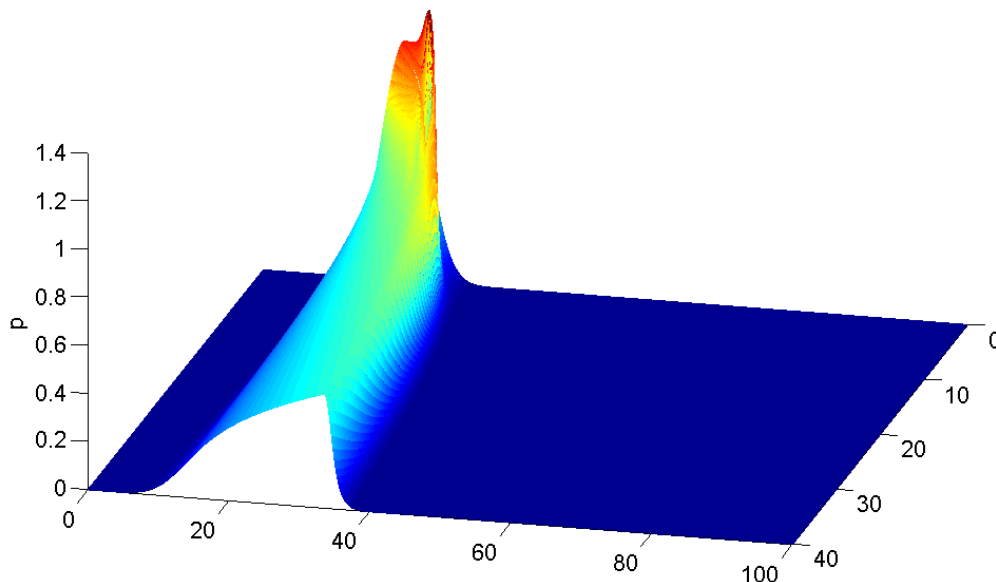


Figure 5 – Acoustic pressure field as a function of space and time for Dirichlet's boundary conditions,  $\mu = 0.1$  and  $\delta = 0.1$ , and a Gaussian initial condition characterized by  $a = 0$ ,  $b = 0.1$  and  $c = 20$

When the medium is a viscous one, the effect of viscosity is to thicken the wave width and decrease its amplitude as illustrated in Figure 5. In addition, the results presented in Figure 5 indicate that the wave's front has a similar structure to those observed in Figures 1 and 2, whereas the back of the wave is more rounded than those of those figures. Figure 5 also shows the complex dynamics at initial times characterized by a drop in amplitude and adjustments from the initial Gaussian shape to that of a decaying weak shock.

## 5 Conclusions

The effects of relaxation on the propagation of one-dimensional acoustic waves have been analyzed by considering the linear momentum equation and introducing a delay or time lag between the velocity gradient and the stress in a Newtonian fluid. Such an approximation results in a modified Burgers' equation that reduces to the original Burgers's equation for zero relaxation times. It has been shown that the resulting equation includes the equal-width and regularized long-wave equations that admit solitary wave solutions. It has also been shown that, for both initial conditions of the Gaussian and sinusoidal types, a shock wave is formed whose

amplitude decreases as the viscosity is increased and that a regular perturbation method may be used to study the wave propagation. In the absence of viscosity, it has been found that there is a steepening of the wave caused by the nonlinear convection terms, and many solitary waves may be formed whenever these nonlinearities are balanced by dispersion. However, when there is viscosity, there is an initial transient during which the initial amplitude decreases and the pressure field adjusts so that a decaying weak shock wave is formed.

### Acknowledgements

The research reported in this paper was supported by Project FIS2012-38430 from the Ministerio de Economía y Competitividad of Spain.

### References

- [1] Bateman, H. Some recent researches on the motion of fluids. *Monthly Weather Rev.*, Vol. 43, 1915, pp. 163-170.
- [2] Burgers, J. M. A mathematical model illustrating the theory of turbulence. *Adv. Appl. Mech.*, Vol. 1, 1948, pp. 171-199.
- [3] Rudenko, O. V. Nonlinear sawtooth-shaped waves. *Physics-Uspekh.*, Vol. 38 (9), 1995, pp. 965-990.
- [4] Nimmo, J. J. C.; Crighton, D. G. Geometrical and diffusive effects in nonlinear acoustic propagation over long ranges, *Phil. Trans. R. Soc. London A*, Vol. 320, 1986, pp. 1-35.
- [5] Hopf, E. The partial differential equation  $u_t + u u_x = u_{xx}$ . *Comm. Pure and Appl. Math.*, Vol. 3, 1950, pp. 201-230.
- [6] Cole, J. D. On a quasi-linear parabolic equation occurring in aerodynamics. *Quartely Appl. Math.*, Vol. 9 (3), 1951, pp. 225-236.
- [7] Peregrine, D. H. Calculations of the development of an undular bore, *J. Fluid Mech.*, Vol. 25, 1966, pp. 321-330.
- [8] Fay, R. D. Plane sound waves of finite amplitude. *J. Acoust. Soc. Am.*, Vol. 3 (2<sup>a</sup>), 1931, pp. 22-241.
- [9] Rudenko, O. V.; Soluyan, S. I. *Theoretical foundations of nonlinear acoustics*. Consultants Bureau, New York, 1977, pp. 88-96.
- [10] Pierce, A. D. *Acoustics: An introduction to its physical principles and applications*. Acoustical Society of America, New York, 1989, pp. 588-591.
- [11] Polyakova, A. L.; Soluyan, S. I.; Khokhlov, R. V. Propagation of finite disturbances in a relaxing medium. *Sov. Phys. Acoust.*, Vol. (1), 1962, pp. 78-82.
- [12] Hamilton, M. F.; Morfey, C. L. Model equations, in: M. F. Hamilton and D. T. Blackstock (eds.), *Nonlinear Acoustics*, pp. 41-63, Academic Press, New York, 1997.
- [13] Ramos, J. I. Solitary waves of the EW and RLW equations. *Chaos, Solitons & Fractals*, Vol. 34 (5), 2007, pp. 1498-1518.
- [14] Ramos, J. I. Solitary wave interactions of the GRLW equation. *Chaos, Solitons & Fractals*, Vol. 33 (2), 2007, pp. 479-491.
- [15] Ramos, J. I. Implicit, compact, linearized  $\theta$ -methods with factorization for multidimensional reaction-diffusion equations. *Applied Mathematics and Computation*, Vol. 94 (1), 1998, pp. 17-43.